Asian Journal of Chemistry; Vol. 29, No. 12 (2017), 2743-2749

ASIAN JOURNAL OF CHEMISTRY

https://doi.org/10.14233/ajchem.2017.20860

Isothermal Study on Removal of Methyl Red from Aqueous Solution Using *Aloe vera* Leaves Powder

RENU SAXENA and SAPNA SHARMA*

Department of Chemistry, School of Sciences, JECRC University, JECRC Foundation, Jaipur-303 905, India

*Corresponding author: E-mail: drsharmasapna@gmail.com

Received: 14 June 2017; *Accepted*: 17 August 2017; *Published online*: 30 October 2017; AJC-18626

The potentiality of *Aloe vera* leaves powder (ALP) a low cost and eco-friendly adsorbent was characterized and investigated for the removal of methyl red dye from an aqueous solution using a green approach by the process of adsorption. The adsorption behaviour of the biosorbent was investigated by performing both kinetic and equilibrium isothermal studies in batch conditions at 34 ºC. Adsorption experiments were performed by changing different experimental parameters *i.e.*, contact time, initial dye concentration, adsorbent dose, particle size and pH of the solution. The adsorption studies were best fitted with Langmuir isotherm and it gives monolayer adsorption capacity of 51.49 mg/g at pH 4.2 at 34 ºC. The correlation coefficient values indicate a moderate fit for monolayer Langmuir model (R^2 = 0.99). The experimental and calculated values for amount of adsorbed dye per unit mass of sorbent (q_e) for pseudo-second-order kinetic model were in good agreement as compared to that by pseudo first order kinetics. The structural characterization of *Aloe vera* leaves powder was performed by SEM, FTIR and by GC-MS.

Keywords: *Aloe vera*, Methyl red dye, Adsorption study, Correlation coefficient, Isotherm models, Kinetics.

INTRODUCTION

With increasing of generation of technologies, water pollution is continuing a great concern problem. With day by day collective amount of dyes in the water received from fast activities of textile industries and as a result humans and animals are facing various problems along with aquatic environment [1]. As dyes are broadly used in industries such as textile, paper, plastic and leather for the coloration of products, the effluents emanating from these industries often contain high concentrations of dye wastes [2]. Synthetic dyes can cause considerable environmental pollution and are serious health hazards [3].

Various techniques have been employed for the treatment of dye bearing industrial effluents. It includes precipitation, adsorption, ion exchange [4], ion exchange membrane process [5], and electro chemical technologies [6]. All of these methods have its own drawback and limitations [7].Therefore, the search for efficient, eco-friendly and cost effective remedies for waste water treatment have been initiated [8]. Now a days, research attention has been focused on environment friendly methods for the treatment of effluents [9]. Bioadsorption is one of the methods that do not require energy and the processes can be carried out *in situ* at the contaminated site and also they are cost effective [10]. In these adsorption methods, plant materials were used as biosorbents for the removal of toxic dyes and metals through adsorption [11]. Plant materials are mainly comprised of cellulose materials that can adsorb dyes in aqueous solution [12]. Numerous waste biomass sources are available in nature in which adsorption properties have been reported such as bagasse pith [13], sawdust [14], rice husk [15], eucalyptus bark [16], fly ash [17], hazelnut shell [18], *etc*.

Scientific investigations on *Aloe vera* have gained more attention over the last several decades due to its several medicinal properties [19]. *Aloe vera* has a long history as a medicinal plant with diverse therapeutic applications. The plant *Aloe vera*, belongs to the family Liliaceae and is a cactus-like perennial plant [20]. The genus Aloe contains over 400 different species with *Aloe barbadensis* Miller [21]. The *Aloe vera* plant has been known and used for centuries for its health, beauty, medicinal and skin care properties [22]. In the present study, *Aloe vera* leaves powder was studied as a new sorbent for the removal of azo dye, methyl red from aqueous solutions by adsorption under various conditions like pH, adsorbent dose, agitation time and particle size.

EXPERIMENTAL

The instruments used in this work include spectrophotometer (Digital UV Spectrophotometer, Model UV 2300, Chemito make), Digital pH meter (Electronic India, EI Model 112), Standard test sieve (MSECO Maharani Scientific and Engin-

eering Cooperation, Delhi) and orbital shaker (Remi Instrument Ltd., IHB, 597).

Adsorbate: An azo dye methyl red, having pH 4.2, *m.f.* $C_{15}H_{15}N_3O_2$, m.w. 269.30 g/mol, m.p. 180 °C was purchased from Merck Ltd., India. The methyl red show maximum absorption at wavelength 525 nm.

Adsorbent: Mature *Aloe vera* leaves collected from a local park of Jaipur city, India. *Aloe vera* leaves were washed with distilled water to clean it thoroughly. They were then cut into small pieces and allowed to dry at room temperature in a shadow for 2-3 weeks. Leaves were then kept in an air oven at 60 to 70 ºC for 3 h till the leaves became brittle. The dried leaves were then grinded by mechanical grinder to convert into fine powder. The powder was sieved to different particle size of 500, 300 and 150 µ for the decolorization experiments. Finally, the product was stored in vacuum desiccators until required. The powder so obtained was named as *Aloe vera* leaves powder (ALP). No other chemical or physical treatments were used prior to adsorption experiment.

Biosorption studies: The batch sorption experiments were carried out in 250 mL Erlenmeyer flask where 0.10 g of adsorbent (*Aloe vera* leaves powder) and 30 mL methyl red dye solution (100-500 ppm) at pH 4.2 were added at 34 ºC. The pH of solution was maintained by adding 1N NaOH and 1 N HCl solutions. The Erlenmeyer flask was capped and agitated in an isothermal shaker at 100 rpm at 34 ºC for 4 h to achieve equilibrium. The concentration of dye in solution after equilibrium adsorption was determined by UV-visible spectrophotometer at 525 nm. The amount of adsorption at equilibrium (q_e, mg/g), was calculated as follows:

$$q_e = \frac{(C_o - C_e)V}{W} \quad (1)$$

where C_o and C_e (mg/L) are the liquid-phase concentration of dye at initial and equilibrium state, respectively. V is the volume of the solution (L) and W is the mass of dry adsorbent (g).

Kinetic studies of adsorption were also carried out at various concentrations of methyl red and the extent of adsorption was investigated as a function of time. The amount of adsorption (q_t, mg/g) at time t, was calculated as:

$$q_t = \frac{(C_o - C_t)V}{W} \quad (2)$$

RESULTS AND DISCUSSION

SEM: Fig. 1(a-b) shows the scanning electron microscopy micrographs of *Aloe vera* leaves powder sample before adsorption of methyl red and *Aloe vera* leaves powder loaded with methyl red. The *Aloe vera* leaves powder exhibited uneven and cave like rough surface morphology. The surface of dye loaded adsorbent indicates that some of the surface of *Aloe vera* leaves powder was covered with dye molecules. The uneven surface of methyl red loaded *Aloe vera* leaves powder show that various functional groups present on adsorbate and adsorbent play important role in the process of adsorption.

The GC-MS spectra (Fig. 2) for *Aloe vera* leaves powder show major peak on relative abundance 27.11 of 6-methyl-*s*-methylene-2-heptanone and two other major compounds are 2,2,5-trimethyl-3,4-hexanedione and 1-*tert*-butyl-3,3-*bis* (trifluoromethyl)diaziridine with relative abundance 24.24 and

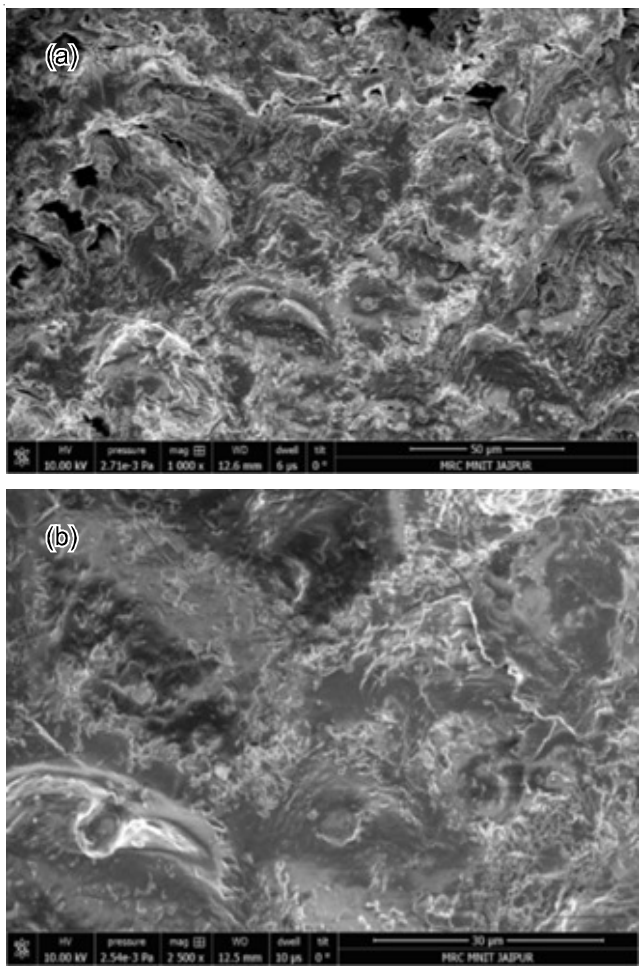

Fig. 1. SEM micrographs of (a) fresh ALP and (b) MR adsorbed ALP

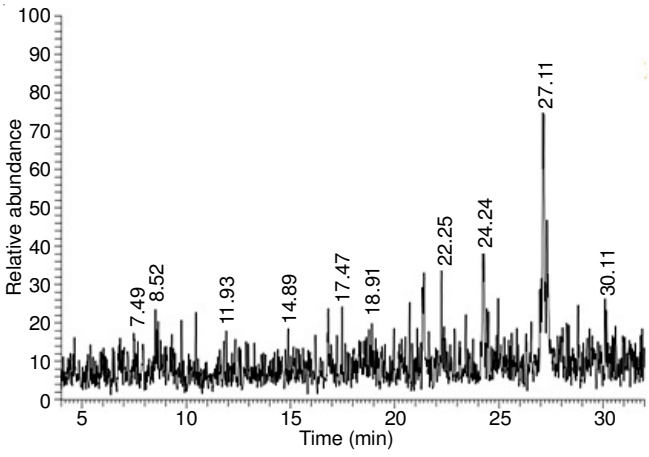

Fig. 2. GC-MS of ALP

22.25, respectively. Other peaks are due to other minor compounds present in *Aloe vera* leaves powder.

Characterization of ALP through FTIR: Fourier transform infrared (FTIR 2000, Perkin, Elmer) analysis were applied on methyl red dye adsorbed ALP to determine the surface functional groups. After dye adsorption, it has been cleared that some peaks has been eliminated and some has been reduced in its peak length as many sorption sites occupied due to adsorption. The FTIR spectrum of ALP is shown in Fig. 3a. Spectra show its following peaks at 3339.75 cm^{-1} (N-H stretching in amines and amides), 2926 cm^{-1} (C-H stretching in alkanes), 1716 cm^{-1} (C=O

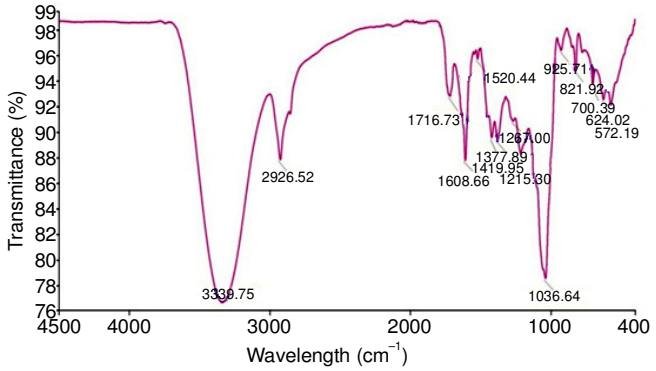

Fig. 3(a). FTIR of fresh ALP

stretching in aldehydes and saturated aliphatic group), 1608 cm^{-1} (N-H bending in amines),1036 cm^{-1} (N-O stretching in nitro compounds), 700 cm^{-1} (shows alkynes groups). It was found that *Aloe vera* leaves powder show large fluctuations in polysaccharide composition. It has been found that the composition of aloe parenchyma tissue or pulp are proteins, lipids, amino acids, vitamins, enzymes, inorganic compounds and small organic compounds in addition to the different carbohydrates [23].The mannosyl residues present in a reserve polysaccharide with a significant seasonal influence [24].

Fig. 3b shows FTIR spectra for methyl red adsorbed ALP. The spectra show the peaks at 3434.94 cm^{-1} (due to stretching in O-H group, alcohol, phenol group), 2924.89 cm^{-1} (C-H stretching in alkene group) and 2853 cm^{-1} (C-H stretch, alkane), 1735 cm^{-1} (C=O stretching in ester and saturated aliphatic group), 1613 cm^{-1} (N-H bending in amines), 1439 cm^{-1} (C-C stretching in ring in aromatics group), 1052 cm^{-1} (C-O stretching in alcohol and carboxylic acids). It is clear that the biosorbent displays a number of sorption peaks, showing the complex nature of adsorbent. FTIR spectra show that the hydroxyl and carbonyl groups are the main functional groups which are present on the surface of the biosorbent and are involved in the process of biosorption. Comparing the spectra, significant changes were observed which shows that these groups play significant role in adsorption.

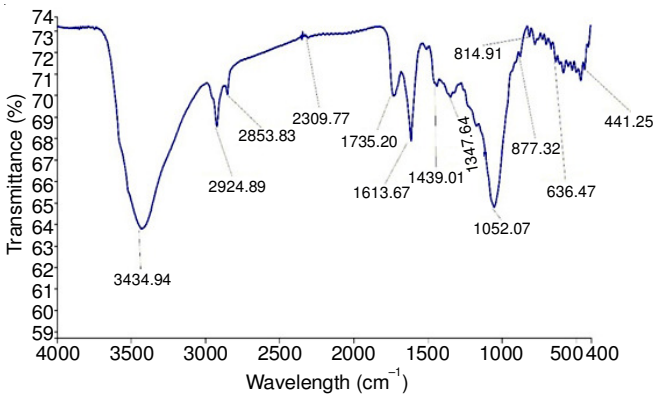

Fig. 3(b). FTIR of ALP loaded with MR dye

Effect of initial concentration on dye adsorption: The effect of initial methyl red concentration (100-500 ppm) on the intake rate by ALP adsorption at adsorbent dosage of 0.10 g and mixing speed of 110 rpm is shown in Fig. 4. It can be seen that the adsorption at different concentration is gradually

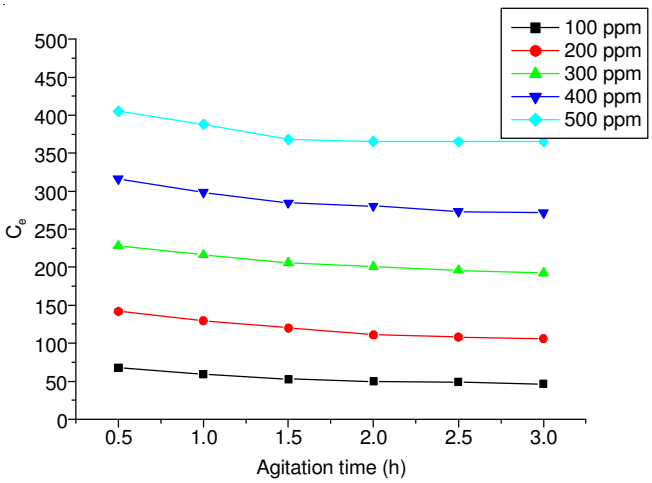

Fig. 4. Effect of initial dye concentration on removal of MR by ALP (conditions: sorbent dosage (W), 0.10 g; initial pH, 4.2; temperature, 34 °C; particle size, 500 µ; stirring rate, 110 rpm; V, 30 mL)

decreases with the progress of adsorption until the equilibrium is reached.The amount of methyl red dye adsorbed at equilibrium (q_e) increased from 16.11 to 40.5 mg/g, as the concentration of dye was increased from 100 to 500 ppm. The initial dye concentration generates a driving force to overcome all mass transfer resistances of the dye between the aqueous and solid phase. Hence, a higher initial concentration of dye will enhance the adsorption process. The methyl red removal decreased from 53.7 to 27 % as methyl red concentration was increased from 100 to 500 ppm .The equilibrium conditions were reached within 3 h.

Results shows that the percentage of dye removal decreases on increasing initial concentration of methyl red dye. Fig. 5 shows the plot between initial dye concentration and the percentage of the dyes removed.

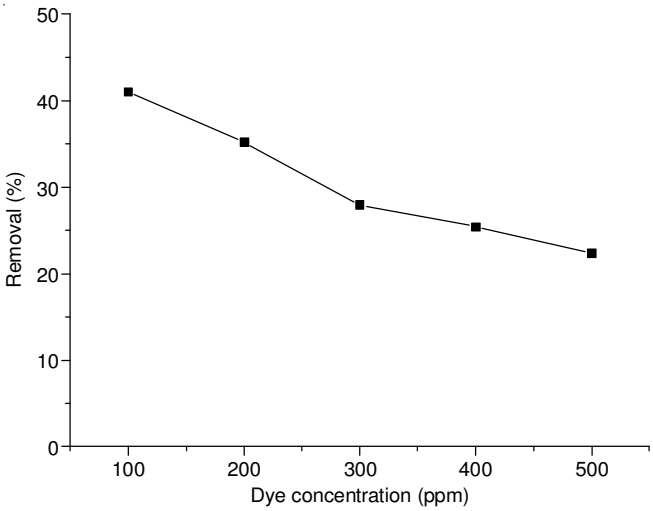

Fig. 5. Effect of initial dye concentration on percentage removal of MR by ALP (conditions: sorbent dosage (W), 0.10 g; initial pH, 4.2; temperature, 34 °C; particle size, 500 µ; stirring rate, 110 rpm; V, 30 mL; dye concentration,100-500 ppm; agitation time, 1 h)

Effect of pH on adsorption: The effect of pH on adsorption was studied using 100 ppm dye concentration, dosage 0.10 g, pH 2 -10 at 34 ºC. Dye removal increased from 22.3 to 41 % as pH increases 2 to 4, then it decreases from 41 to 34.2 % as

pH further increases to 10 (Fig. 6).The q_e was found to increase with increasing pH from 6.69 to12.3 mg/g and decreases upto 10.26 mg/g. In acidic medium, the positive charge increases on the adsorbent surface causing an increase in the electrostatic attraction between anionic dye molecules and the surface of adsorbents so there is an increased rate of adsorption of the dye. On the other hand as concentration of hydroxyl ions (OH^-) on the adsorbents increases, it compete effectively with the dye molecules leading to decreased percent adsorption onto the surface of adsorbent.

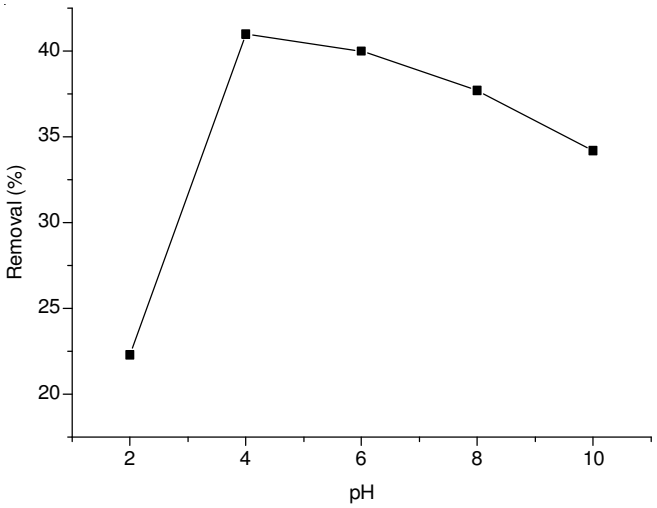

Fig. 6. Effect of solution pH on percentage removal of MR by ALP (conditions: sorbent dosage (W), 0.10 g; initial pH, 4.2; temperature, 34 °C; particle size, 500 µ; stirring rate, 110 rpm; V, 30 mL; dye concentration, 100 ppm; agitation time, 1h)

Effect of biosorbent dose on adsorption: The experiments were conducted with constant dye concentration (100 ppm) and samples with different biosorbent dosages ranging from 0.10 to 0.25 g under constant temperature at 34 ºC and pH 4.2 for 1 h. It was observed that percentage of dye adsorption increased with increase of adsorbent dose. The removal of dye increases from 21 to 57 % with the increase of sorbent dose from 0.05 to 0.25g. This is mostly due to an increase in the adsorption surface area and the availability of more active available sites. In Fig. 7, the slope is positive, which indicates that adsorption increases with an increase in adsorption dose. It is clear that a certain amount of dye is adsorbed by a fixed mass of the adsorbent.

Effect of particle size on biosorption: Percentage removal of dye increases on decreasing particle size. It is due to the reason that more fine powder increases the surface area for adsorption. On reducing particle size from 500 to 150 µ, percentage removal increases from 41 to 59.7 % (Fig. 8).

Effect of agitation time on adsorption: Batch equilibrium studies were carried out by adding fixed amount of sorbent 0.10 g to 100 ppm dye solution at 4.2 pH at 34 ºC (Fig. 9). Aliquots were agitated in shaker at 110 rpm at different constant time (0.5, 1.0, 1.5, 2.0, 2.5 and 3.0 h) and concentrations were analyzed. Due to higher contact time, percentage removal of dye increases. On increasing agitation time from 0.5 to 3 h, percentage removal of dye increases from 32 to 53.7 %.

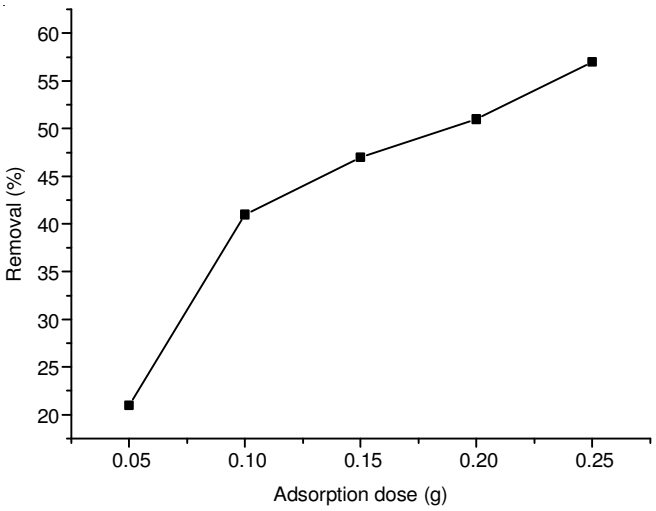

Fig. 7. Effect of biosorbent dosage (g) on percentage removal of MR by ALP (conditions: initial pH, 4.2; temperature, 34 °C; particle size, 500 µ; stirring rate, 110 rpm; V, 30 mL; Dye concentration, 100 ppm, time, 1 h)

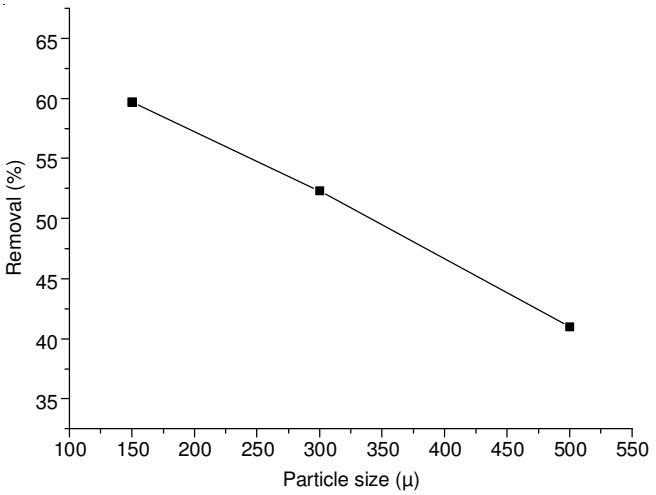

Fig. 8. Effect of particle size on percentage removal of MR by ALP (conditions: sorbent dosage (W), 0.10 g; initial pH, 4.2; temperature, 34 °C; stirring rate, 110 rpm; V, 30 mL; Dye concentration, 100 ppm; Agitation time, 1 h)

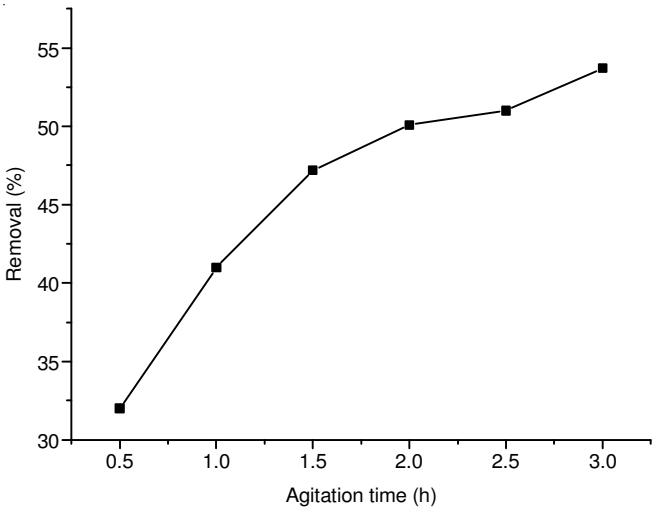

Fig. 9. Effect of agitation time on percentage removal of MR by ALP (conditions: sorbent dosage (W), 0.10 g; initial pH, 4.2; temperature, 34 °C; stirring rate, 110 rpm; V, 30 mL; Dye concentration, 100 ppm)

Adsorption isotherms: The adsorbate concentration in bulk and adsorbed amount at the interface can be related by means of adsorption isotherms. The isotherm results were analyzed using Langmuir and Freundlich isotherms. The Langmuir adsorption model [25] is based on the assumption that maximum adsorption corresponds to a saturated monolayer of solute molecules on the adsorbent surface, with no later interaction between the sorbed molecules.The expression of the Langmuir model is given as follows:

$$q_e = \frac{Q_o b C_e}{(1 + bC_e)} \quad (3)$$

where q_e (mg/g) and C_e (mg/L) are the amount of adsorbed dye per unit mass of sorbent and unadsorbed dye concentration in solution at equilibrium, respectively. Q_o is the maximum amount of the dye per unit mass of sorbent to form a complete monolayer on the surface bound at high C_e, and b is a constant related to the affinity of binding sites (L/mg).The Langmuir equation can be described by the linearized forms shown in eqn. 4:

$$\frac{C_e}{q_e} = \frac{1 + C_e}{Q_o} \quad (4)$$

A graph between specific adsorption C_e/q_e against equilibrium concentration C_e gives linear plot (Fig. 10), which shows that the adsorption obeys the Langmuir model. The Langmuir constants Q_o and b were determined from the slope and intercept of the plot. The essential characteristic of Langmuir isotherm can be expressed in term of a dimensionless constant separation factor R_L which is given as follows:

$$R_L = \frac{1}{(1 + bC_o)} \quad (5)$$

where C_o is highest initial concentration of adsorbate (mg/L or ppm) and b (L/mg) is Langmuir constant. The value of R_L indicates the shape of the isotherms to be either unfavourable ($R_L > 1$), linear ($R_L = 1$), favorable ($0 < R_L < 1$), or irreversible ($R_L = 0$). In present study, value of R_L comes out to be 0.166 for adsorption of methyl red dye onto ALP. Further, the investigation was correlated with value of correlation coefficient. The study shows value of correlation coefficient (R^2) as 0.997.

The Freundlich isotherm [26] describes heterogeneous system by eqn. 6:

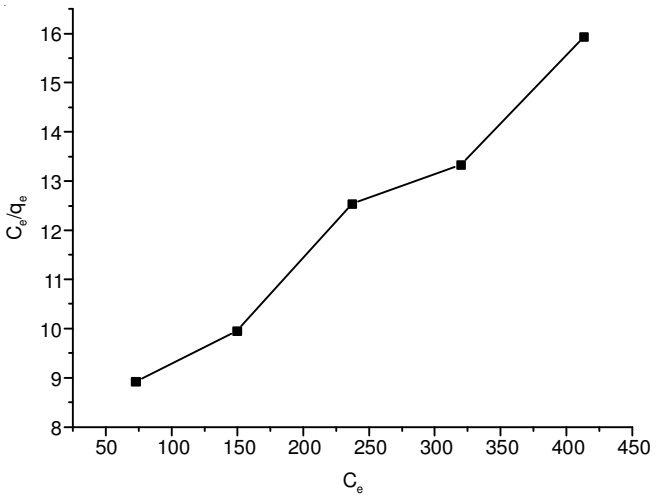

Fig. 10. Langmuir Model curve for MR sorption onto ALP at 34 °C

$$q_e = K_F C_e^{1/n} \quad (6)$$

where K_F and n are Freundlich constant. K_F [mg/g (L/mg)$^{1/n}$] is the adsorption capacity of the sorbent and n gives an indication of favourable adsorption process. The magnitude of exponent, 1/n, gives an indication of favorability of adsorption. Value of $n > 1$ represent favourable adsorption condition [27]. To determine the constants K_F and n, the linear form of the equation used to produce a graph of ln q_e against ln C_e (Fig. 11). Value of K_F and n are calculated from the intercept and slope of the plot using eqn. 7:

$$\ln q_e = \ln K_F + \left(\frac{1}{n}\right) \ln C_e \quad (7)$$

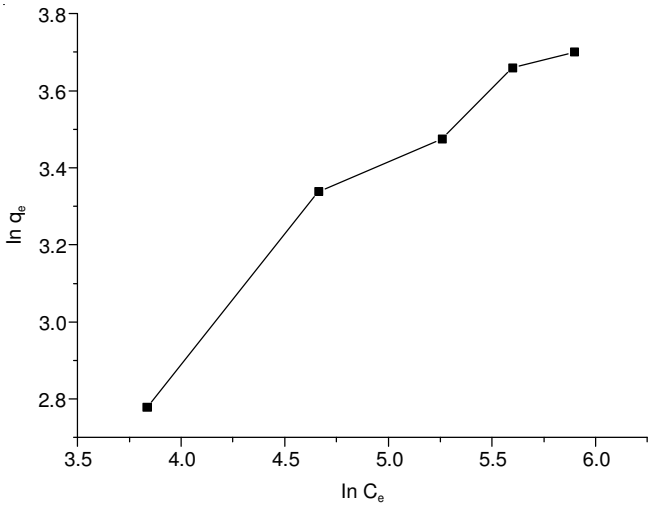

Fig. 11. Freundlich model curve for MR sorption onto ALP at 34 °C

The value of R^2 according to Freundlich isotherm comes out to be 0.968. The results for various isotherms are shown in Table-1.

TABLE-1
LANGMUIR AND FREUNDLICH MODEL CONSTANTS AND CORRELATION COEFFICIENT FOR BIOSORPTION OF MR ONTO ALP

Langmuir isotherm	Isotherm parameters	Freundlich isotherm	Isotherm parameters
Q_o (mg/g)	51.49	K_F	3.17
b (L/mg)	0.010	n	2.26
R^2	0.997	R^2	0.968
R_L	0.166	–	–

As shown in Table-1, the Langmuir isotherm is quite fit well with the experimental data as correlation coefficient R^2 is 0.997. But in case of Freundlich isotherm, the correlation coefficient R^2 is less than 0.99, which show less agreement with experimental data. The monolayer adsorption capacity according to Langmuir model was 51.49 mg/g. The Langmuir isotherm fit well because of homogeneous distribution of active sites onto ALP surface.

Adsorption kinetics: Adsorption kinetics was studied with pseudo-first-order model which was explained by Lagergren [28] as in eqn. 8:

$$\log (q_e - q_t) = \log q_e - \frac{k_1 t}{2.303} \quad (8)$$

A linear plot of log ($q_e - q_t$) against time allows one to obtain the rate constant (Fig. 12). If the plot was found to be linear with good correlation coefficient, then it indicates that Lagergren's equation is appropriate to methyl red dye sorption on ALP. The results of Lagergren's first order rate constant (k_1) and q_e determined from the model are presented in Table-2 along with the corresponding correlation coefficients. It was found that the calculated q_e values do not agree with the experimental q_e values which further suggest that the adsorption of methyl red dye do not follow first-order kinetics.

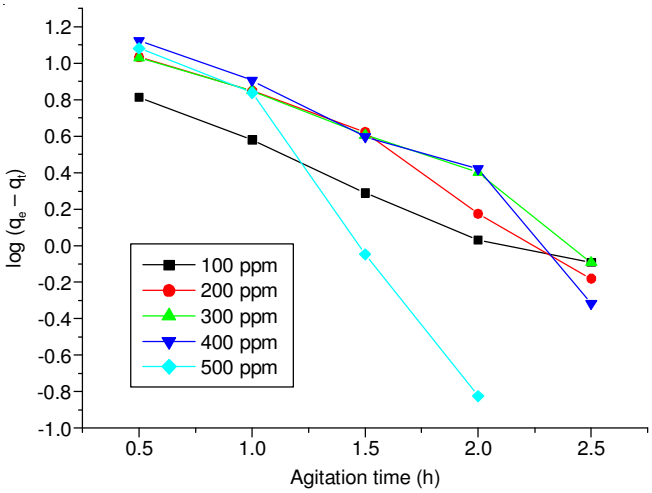

Fig. 12. Pseudo-first-order adsorption kinetics of MR onto ALP

The pseudo second-order kinetics [29] can be expressed in a linear form as follows:

$$\frac{t}{q_t} = \frac{1}{k_2 q_e^2} + \frac{1}{q_e} t \quad (9)$$

where the equilibrium adsorption capacity (q_e), and the second order constants k_2 (g/mgh) can be determined experimentally from the slope and intercept of plot t/q_t *versus* t (Fig.13). The k_2 and q_e determined from the second order model are presented in Table-2 along with the corresponding correlation coefficients. There is an agreement between q_e experimental and q_e calculated

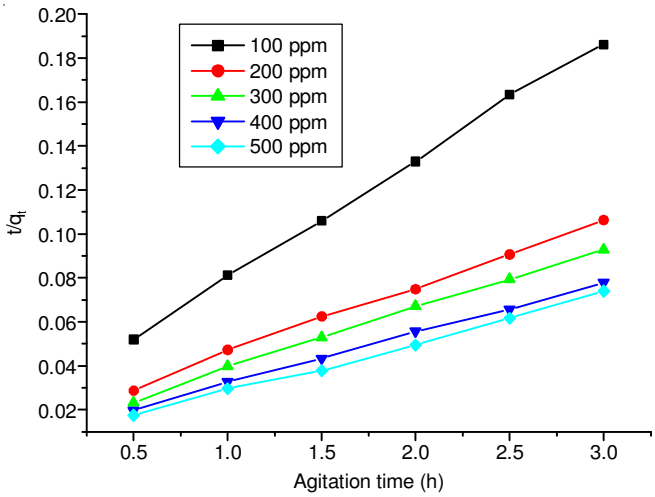

Fig. 13. Pseudo second-order adsorption kinetics of methyl red dye onto ALP

values for the pseudo second-order model. The value of correlation coefficient R^2 = 0.99 which further indicates that pseudo second-order model better represented the adsorption kinetics and kinetics rate depends on both adsorbent and adsorbate concentration.

Similarly, the kinetic study of methyl red dye on activated carbon prepared from *Annona squmosa* seed was analyzed based on pseudo first-order and pseudo second-order. The data indicates that the adsorption kinetics follow the pseudo second-order [30].

Adsorption capacity of ALP has been compared with various other biosorbents. On comparing the adsorption capacity of ALP with other biosorbents (Table-3), it can be concluded that ALP could be used as better biosorbent.

Conclusion

In the present investigation, the adsorption ability of *Aloe vera* leaves powder (ALP) to remove methyl red dye from aqueous solution was investigated. Variation in various parameters *viz*., initial dye concentration, biosorbent concentration, pH of solution was conducted during experimental work. Decolourization

TABLE-2
COMPARISON OF THE PSEUDO-FIRST-ORDER, PSEUDO-SECOND-ORDER ADSORPTION RATE CONSTANT AND CALCULATED AND EXPERIMENTAL q_e VALUES OBTAINED AT DIFFERENT INITIAL MR CONCENTRATION

Conc. initial (mg/L)	Pseudo-first order kinetic model				Pseudo-second-order kinetic model		
	q_e exp (mg/g)	K_1 (1/h)	q_e cal (mg/g)	R^2	K_2 (g/mg h)	q_e cal (mg/g)	R^2
100	16.11	-1.08586	10.78191	0.9857	0.11247	18.53911	0.9991
200	28.20	-1.42859	26.9882	0.9716	0.07985	28.5715	0.9975
300	32.31	-1.24744	23.7463	0.9565	0.06825	36.3755	0.9979
400	38.52	-1.55222	36.0843	0.9237	0.07428	38.4615	0.9994
500	40.50	-3.04000	81.8452	0.9562	0.08802	43.4782	0.9967

TABLE-3
COMPARISON FOR ADSORPTION CAPACITY OF DIFFERENT BIOSORBENTS FOR REMOVAL OF MR DYE

Biosorbent used	Adsorption capacity (mg/g)	Reference
Algerian bentonite-type clay from Mostaganem region (MBC)	2.0	[31]
Neplhelium lappaceum seed	4.446	[32]
Modified banana trunk fibers (BTF)	8.74	[33]
Banana Pseudostem Fibers	17.25	[34]
Annona squmosa seed	40.486	[30]
Aloe vera leaves powder (ALP)	51.49	Present study

experiments were also performed with respect to agitation time and particle size. Adsorption modeling of experimental data was conducted through Langmuir and Frendulich isotherm model. It is found that Langmuir adsorption isotherm fitted well with monolayer adsorption capacity as 51.49 mg/g at pH 4.2 at 34 ºC and show better correlation coefficient as 0.997 as compared to that obtained through Frendulich isotherm. This is because of effective inter-actions of various active groups on *Aloe vera* leaves powder with methyl red dye. Results for kinetic study are in well agreement for pseudo second-order kinetic equation ($R^2 > 0.99$) conclude that *Aloe vera* leaves powder could be used as one of the low cost biosorbent for removal of methyl red dye from aqueous solutions.

ACKNOWLEDGEMENTS

One of the authors, (RS) acknowledge the research grant provide by Vice-Chairman of JECRC University, for her research work. The authors acknowledge to President, JECRC University, for providing laboratory facilities. Thanks are also due to SEED, Department of Science and Technology, New Delhi for providing WTP (Women Technology Park) to JECRC and financial support.

REFERENCES

1. N. Ahalya and T.V. Ramachandra, Restoration of Wetlands-Feasibility Aspects of Biological Restoration, The National Conference, Coimbatore, India (2002).
2. G.S. Gupta, S.P. Shukla, G. Prasad and V.N. Singh, *Environ. Technol.*, **13**, 925 (1992); https://doi.org/10.1080/09593339209385228.
3. E. Forgacs, T. Cserháti and G. Oros, *Environ. Int.*, **30**, 953 (2004); https://doi.org/10.1016/j.envint.2004.02.001.
4. P.K. Sinha, R.V. Amalraj and V. Krishnasamy, *Radiochim. Acta*, **65**, 125 (1994); https://doi.org/10.1524/ract.1994.65.2.125.
5. A.F. Nechaev, V. Projaev and V.P. Kapranchik, Radioactive Waste Management and Environmental Remediation, Int. Conference, American Society of Mechanical Engineers, New York, p. 1145 (1995).
6. A. Szygula, E. Guibal, M.A. Palacín, M. Ruiz and A.M. Sastre, *J. Environ. Manage.*, **90**, 2979 (2009); https://doi.org/10.1016/j.jenvman.2009.04.002.
7. S.M. Ghoreishi and R. Haghighi, *Chem. Eng. J.*, **95**, 163 (2003); https://doi.org/10.1016/S1385-8947(03)00100-1.
8. Z. Aksu, *Process Biochem.*, **40**, 997 (2005); https://doi.org/10.1016/j.procbio.2004.04.008.
9. A. Gurses, C. Dogar, M. Yalcin, M. Acikyildiz, R. Bayrak and S. Karaca, *J. Hazard. Mater.*, **131**, 217 (2006); https://doi.org/10.1016/j.jhazmat.2005.09.036.
10. I. Michalak, K. Chojnacka and A. Witek-Krowiak, *Appl. Biochem. Biotechnol*., **170**, 1389 (2013); https://doi.org/10.1007/s12010-013-0269-0.
11. S.J.T. Pollard, G.D. Fowler, C.J. Sollars and R. Perry, *Sci. Total Environ.*, **116**, 31 (1992); https://doi.org/10.1016/0048-9697(92)90363-W.
12. A.J. Varma, S.V. Deshpande and J.F. Kennedy, *Carbohydr. Polym.*, **55**, 77 (2004); https://doi.org/10.1016/j.carbpol.2003.08.005.
13. Y.S. Ho and G. McKay, *Process Biochem.*, **38**, 1047 (2003); https://doi.org/10.1016/S0032-9592(02)00239-X.
14. V.K. Garg, M. Amita, R. Kumar and R. Gupta, *Dyes Pigments*, **63**, 243 (2004); https://doi.org/10.1016/j.dyepig.2004.03.005.
15. G. McKay, J.F. Porter and G.R. Prasad, *Water Air Soil Pollut.*, **114**, 423 (1999); https://doi.org/10.1023/A:1005197308228.
16. L.C. Morais, O.M. Freitas, E.P. Gonçalves, L.T. Vasconcelos and C.G. González Beça, *Water Res.*, **33**, 979 (1999); https://doi.org/10.1016/S0043-1354(98)00294-2.
17. P. Janos, H. Buchtova and M. Ryznarova, *Water Res.*, **37**, 4938 (2003); https://doi.org/10.1016/j.watres.2003.08.011.
18. S. Aygün, S. Yenisoy-Karakas and I. Duman, *Micropor. Mesopor. Mater.*, **66**, 189 (2003); https://doi.org/10.1016/j.micromeso.2003.08.028.
19. K. Eshun and Q. He, *Crit. Rev. Food Sci. Nutr.*, **44**, 91 (2004); https://doi.org/10.1080/10408690490424694.
20. A. Surjushe, R. Vasani and D.G. Saple, *Indian J. Dermatol.*, **53**, 163 (2008); https://doi.org/10.4103/0019-5154.44785.
21. A. Bozzi, C. Perrin, S. Austin and F.A. Vera, *Food Chem.*, **103**, 22 (2007); https://doi.org/10.1016/j.foodchem.2006.05.061.
22. M.Z. Haque, M.B. Islam, M.A. Jalil and M.Z. Shafique, *IOSR J. Appl. Chem.*, **7**, 36 (2014); https://doi.org/10.9790/5736-07613640.
23. G.R. Waller, S. Mangiafico and C.R. Ritchey, *Proc. Okla. Acad. Sci.*, **58**, 69 (1978).
24. A. Femenia, P. García-Pascual, S. Simal and C. Rosselló, *Carbohydr. Polym.*, **51**, 397 (2003); https://doi.org/10.1016/S0144-8617(02)00209-6.
25. J. Eastoe and J.S. Dalton, *Adv. J. Colloid Interface Sci.*, **85**, 103 (2000); https://doi.org/10.1016/S0001-8686(99)00017-2.
26. H. Freundlich, *Z. Phys. Chem.*, **57U**, 385 (1907); https://doi.org/10.1515/zpch-1907-5723.
27. V.J.P. Poots, G. McKay and J.J. Healy, *J. Water Pollut. Contr.*, **50**, 926 (1978).
28. S. Lagergren, *K. Sven. Vetenskapsakad. Handl.*, **24**, 1 (1898).
29. Y.S. Ho and G. McKay, *Chem. Eng. J.*, **70**, 115 (1998); https://doi.org/10.1016/S0923-0467(98)00076-1.
30. T. Santhi, S. Manonmani and T. Smitha, *Chem. Eng. Res. Bull.*, **14**, 11 (2010); https://doi.org/10.3329/cerb.v14i1.3767.
31. K. Boudouara, M. Ghelamallah and H.N. Khemliche, Adsorption of Methyl Red from Aqueous Solutions by Algerian Bentonite Clay, 2nd International Congress on Energy Efficiency and Energy Related Materials (ENEFM2014), Springer, Springer Proceedings in Energy, p. 203 (2014).
32. R. Zein, A.W. Astuti, D. Wahyuni and F. Furqani, *Res. J. Pharm. Biol. Chem. Sci.*, **6**, 86 (2015).
33. M. Rosemal, H.M. Haris and K. Sathasivam, *Arch. Appl. Sci. Res.*, **2**, 209 (2010).
34. M. Rosemal, H.M. Haris and K. Sathasivam, *Am. J. Appl. Sci.*, **6**, 1690 (2009); https://doi.org/10.3844/ajassp.2009.1690.1700.